Recalescence behavior and solidification structure of the undercooled $Fe_{82}B_{17}Si_1$ eutectic alloy*

ZHANG Zhenzhong (张振忠), SONG Guangsheng (宋广生), YANG Gencang (杨根仓) and ZHOU Yaohe (周尧和)

(State Key Laboratory of Solidification Processing, Northwestern Polytechnical University, Xi'an 710072, China)

Received May 31, 1999; revised July 3, 1999

Abstract By cyclic superheating incorporated with glass fluxing denucleation method the $Fe_{82}B_{17}Si_1$ eutectic alloy was undercooled up to $\Delta T = 342$ K. The relations between recalescence behavior and solidification structures were systematically studied in the undercooling range of 6—342 K. Two critical undercoolings were observed: mixed eutectic was the unique growth morphology when the undercooling was less than $\Delta T_1 = 63$ K; but the microstructure transformed to complete undercooled anomalous eutectic when the undercooling was greater than $\Delta T_2 = 164$ K. The two eutectic phases α(Fe,Si) and Fe_2B conformed to the non-reciprocal nucleation effect. The boundary of the coupled zone of α(Fe,Si)-Fe_2B system shifted toward the Fe_2B side, and intersected the eutectic composition line at $\Delta T = 154$ K and $\Delta T = 264$ K, whose valley was at about $\Delta T = 207$ K.

Keywords: high undercooling, eutectic alloy, recalescence, coupled zone.

Recalescence is termed as a steep rise of temperature due to the rapid release of latent heat induced by the rapid crystal growth. It is of great significance to investigate the mechanism of rapid solidification, the nucleation relation of the coupled phases in eutectic, and the coupled zone far from equilibrium by studying the relations between the cooling curves and the solidification microstructures. Since the 1970s Flemings and his collaborators[1—5], Tewari[6] and Wei Bingbo[7—10] have studied the recalescence and the solidification microstructures of undercooled eutectic Ni-Sn, Ni-Mo, Co-Mo, Co-Sn, Co-Sb systems, which showed that in a wide undercooling range only one recalescence event took place in the undercooled binary eutectic alloys containing faceted phase, and with the increase of undercooling the eutectic structures all transformed from regular lamellar eutectic to undercooled anomalous eutectic. Fe-B-Si eutectic alloy is one of the most important soft magnetic materials, however, there has not been any report on the microstructure evolution of this alloy under deep undercooling conditions at present. In this study, the $Fe_{82}B_{17}Si_1$ eutectic alloy was undercooled up to $\Delta T =$ 342K by means of the combination of cyclic superheating and glass fluxing, and the relations between the recalescence behavior and the solidification structures were systematically studied.

1 Experimental procedure

$Fe_{82}B_{17}Si_1$(at%) eutectic alloy[11, 12] was chosen as the experimental alloy. It was prepared by melting 99.7% Fe pellets, 99.999% Si and super low carbon $Fe_{24}B$(wt.%) alloy in an HF

* Project supported by the National Natural Science Foundation of China (Grant No. 59701003) and Aeronautics Fundamental Science Foundation of China (Grant No. 98G53089).

induction oven under the protection of molten glass. Each sample weighing 6 g was subjected to cyclic superheating and glass-fluxing denucleation to obtain deep undercooling in a quartz crucible with 11 mm in diameter and 35 mm in height. The composition of the glass denucleation agent is (wt%) SiO_2 74, ($Na_2O + K_2O$) 15.0, CaO 7, Al_2O_3 2.0, MgO 1.8, Fe_2O_3 0.2. The thermal history of the sample was recorded by a DIY infrared pyrometer, which was calibrated with a standard $PtRh_{30}$-$PtRh_6$ thermocouple under isothermal condition. Metallographic specimens were prepared by cutting the samples through nucleation region in the radial direction and etched with 4% nitric acid solution diluted by alcohol. The microstructures were observed with a JXA - 840/EDS-860-2 scanning electron microscope.

2 Results and discussion

2.1 Cooling curves

Figure 1 shows two typical cooling curves of the $Fe_{82}B_{17}Si_1$ eutectic alloy in different undercooling

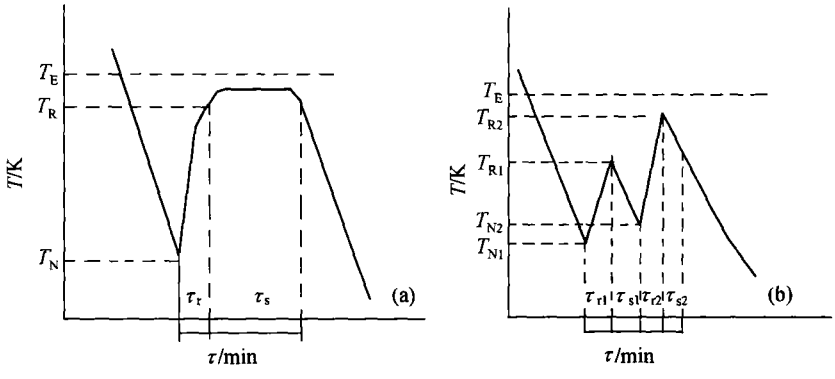

Fig. 1. Typical cooling curves of the $Fe_{82}B_{17}Si_1$ eutectic alloy in different undercooling ranges. (a) ΔT = 6—164 K and 255—342 K; (b) ΔT = 174—247 K.

ranges. There was only one recalescence event for the samples solidified in the undercooling ranges of 6—164 K and 255—342 K as shown in fig.1(a). Their solidification process consisted of an initial rapid solidification stage τ_r along with the recalescence, and a slow solidification period τ_s after the recalescence, where τ_r is the recalescence time, τ_s the slow solidification time. Whereas for the specimens solidified in the undercooling range of 174—247 K, two recalescence events occurred on their cooling curves as shown in fig.1(b); their solidification process consisted of the rapid and slow solidification periods τ_{r1}, τ_{s1} of the primary phase and the accompanying eutectic rapid and slow solidification stages τ_{r2}, τ_{s2}. In fig.1(a), we define T_E as the equilibrium eutectic temperature, T_N the nucleation temperature, T_R the recalescence temperature, $\Delta T_R = T_R - T_N$ the recalescence degree, $V_R = \Delta T_R/\tau_r$ the recalescence rate, $\tau_f = \tau_r + \tau_s$ the total solidification time and $\Delta T = T_E - T_N$ the initial undercooling. In fig.1(b) we define T_{N1}, T_{N2}, T_{R1}, T_{R2} as the nucleation and recalescence temperatures of the primary phase and the eutectic respectively, $\Delta T_{R1} = T_{R1} - T_{N1}$ the first recalescence degree, $\Delta T_{R2} = T_{R2} - T_{N2}$ the second recalescence degree, $\Delta T_R = \Delta T_{R1} + \Delta T_{R2}$ the total recalescence degree, $V_R = \Delta T_{R1}/\tau_{r1}$ the first recalescence rate, $\tau_f = \tau_{r1} + \tau_{s1} + \tau_{r2} + \tau_{s2}$ the total solidification time (the right limits of τ_{r2} and τ_{s2} are defined as the inflexion points of the

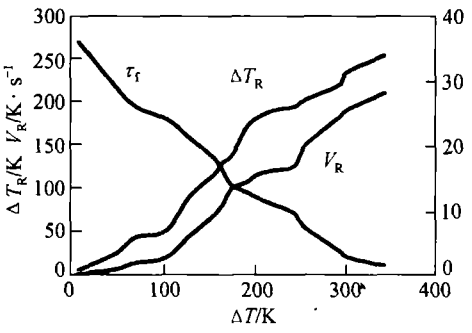

Fig. 2. Influence of initial undercooling ΔT on V_R, ΔT_R and τ_f for undercooled $Fe_{82}B_{17}Si_1$ eutectic alloy.

cooling curve in the second recalescence run[4]) and $\Delta T = T_E - T_{N1}$ the initial undercooling. The influence of initial undercooling on the parameters ΔT_R, V_R and τ_f in the above-mentioned three undercooling ranges is summarized in fig. 2, which shows that with the increase of initial undercooling, the (total) recalescence degree ΔT_R and the (first) recalescence rate increase, but the total solidification time decreases.

2.2 Relation between the recalescence behavior and solidification microstructure

Figures 3(a—d) show the microstructures of the samples with the initial undercoolings of 6, 154, 201 and 255 K respectively, which are typical in the three undercooling ranges. The EDA and XRD results show that the white phase is Fe_2B, and the dark phase is α(Fe,Si) in fig.3. It can be seen that for the samples solidified in the undercooling ranges of 6—164 K and 255—342 K with one recalescence event, the microstructures are mixed eutectic of quasi-regular and complex regular eutectics[13—14] (fig.3(a)) or mixed eutectic plus undercooled anomalous eutectic (fig.3(b)), and complete undercooled anomalous eutectic (fig.3(d)). This indicates that the recalescence in fig.1(a) is caused by the release of latent heat in the eutectic rapid solidification. Croker[13] found that in a binary eutectic system containing faceted phase, the

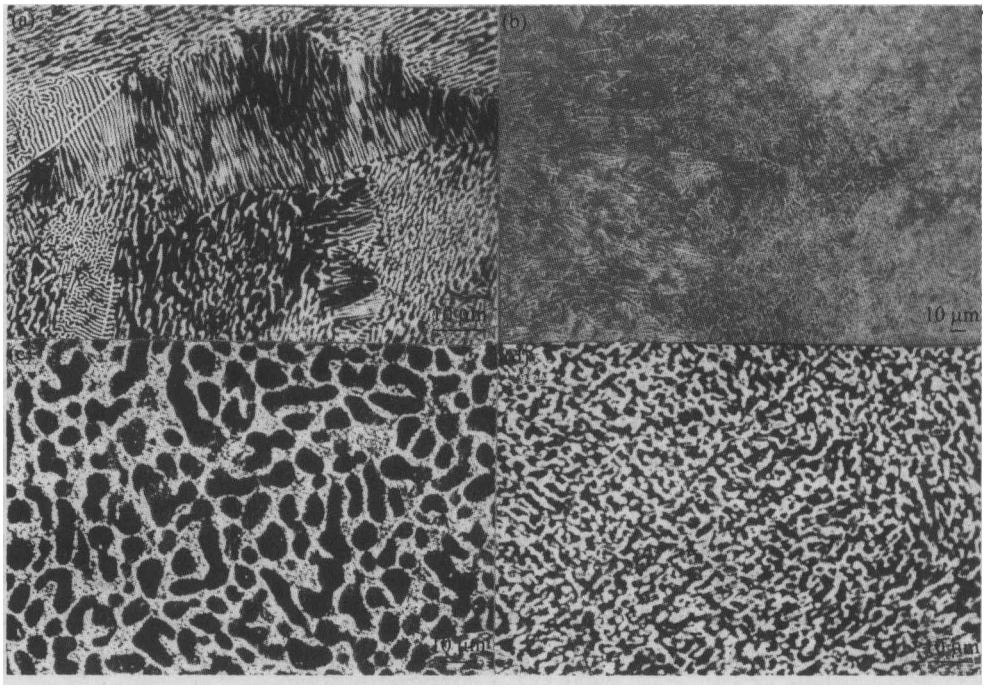

Fig. 3. Typical microstructures in three undercooling ranges for $Fe_{82}B_{17}Si_1$ eutectic alloy. (a) $\Delta T = 6$ K; (b) $\Delta T = 154$ K; (c) $\Delta T = 201$ K; (d) $\Delta T = 255$ K.

microstructure was complex regular eutectic if the volume fraction of faceted phase φ_f was in the range of 20—35%, whereas the microstructure was quasi-regular eutectic structure if $\varphi_f > 40\%$ under the condition that the faceted phase entropy of fusion was beyond 23J/(mol.K). Since in $Fe_{82}B_{17}Si_1$ eutectic alloy the entropy of Fe_2B solution is about 18.1—22.4J/(mol.K)[12], $\varphi_f > 40\%$, it can be deduced that the mixed eutectic structure obtained at lower undercoolings in the alloy is approximately in accordance with the eutectic structure rule summarized by Croker. This is also the main reason why there exists no regular lamellar eutectic structure in the $Fe_{82}B_{17}Si_1$ eutectic alloy. However for the samples solidified in the 174—247 K undercooling range with two recalescence events, the microstructure corresponds to α(Fe,Si) plus interdendrite undercooled anomalous eutectic (fig.3(c)). According to the size and morphology of α phase, it can be inferred that the first recalescence in fig. 1(b) is induced by the rapid solidification of the primary α dendrite phase, whereas the second recalescence is induced by the rapid solidification of the remaining melt growing in the eutectic structure. The influence of initial undercooling and the ratio of two recalescence degrees $\Delta T_{R1}/\Delta T_{R2}$ on the volume fraction of α phase in the undercooling range of 164—255K is summarized in table 1, which indicates that with the increase of initial undercooling, the volume fraction of α phase increases at first and then decreases at $\Delta T = 207$ K, and the higher the $\Delta T_{R1}/\Delta T_{R2}$, the larger is the volume fraction of α phase.

Table 1 Influence of ΔT and $\Delta T_{R1}/\Delta T_{R2}$ on the volume fraction of α phase for $Fe_{82}B_{17}Si_1$ eutectic alloy

Undercooling ΔT/K	164	174	191	207	217	225	238	255
$\Delta T_{R1}/\Delta T_{R2}$	—	0.36	0.83	1.3	0.9	0.8	0.63	—
Volume fraction of α%	~5	~15	35~40	55~60	45~50	30~35	~20	~5

2.3 Non-reciprocal nucleation effect of α(Fe,Si) and Fe_2B phases

Lamplough and Scott[15] found that in a eutectic system of α and β, α usually nucleated β at low undercooling, but β did not nucleate α except at undercooling approaching homogeneous nucleation. Moreover, Sundquist and Mondolfo[16] found that the metals with "complex" structures (having high entropy of fusion) were difficult to nucleate but were good nucleating agents, whereas the metals with simple structures were readily nucleated but were poor nucleating agents after they had detected the nucleation undercooling of two eutectic phases one on the other and had compared the values of entropy of fusion of the two phases in 36 sorts of eutectic systems. This effect was termed as "non-reciprocal nucleation effect". As shown in fig. 3, some Fe_2B phase exhibited the fish-skeleton morphology in the mixed eutectic (fig.3(a)), similarly the Fe_2B phase was in dendrite morphology and the dendrites were connected in the anomalous eutectic (fig.3(b) and (d)). Obviously we could deduce that Fe_2B was the primary phase and was also the proper nucleating agent of α phase in the solidification process of mixed eutectic and undercooled anomalous eutectic structures. By contrast, as shown in fig.1(b) the solidification of eutectic could not occur until a time delay after the α phase nucleated and grew. This result indicated that α(Fe,Si) could not catalyze the nucleation of Fe_2B. Thus we could conclude that the α(Fe,Si) and Fe_2B phases in the deep undercooled $Fe_{82}B_{17}Si_1$ eutectic alloy conformed also to the non-reciprocal nucleation effect.

2.4 Critical undercoolings of undercocled anomalous eutectic

Many experimental results obtained in deep undercooled $Fe_{82}B_{17}Si_1$ eutectic alloy showed that normal nucleation sites were all located at the sample surface, which indicated that the nucleation was heterogeneous nucleation. The rapid solidification process always started from the sample surface, whereas the product of the remaining liquids was generally located in the interior of the sample or at the boundaries of undercooled anomalous eutectic zones. We define the critical undercooling ΔT_1 as the undercooling for the appeareance of undercooled anomalous eutectic at the nucleation point of the sample surface, and the critical undercooling ΔT_2 as the undercooling for the complete transformation of the undercooled anomalous eutectic in all the sample cross-sections. From the experimental results, it could be determined that ΔT_1 was 63 K, and ΔT_2 was 164 K in deep undercooled $Fe_{82}B_{17}Si_1$ eutectic alloy. Fig.4(a—c) show the interior microstructures of the samples with the initial undercooling of 6 K, 107 K and 164 K respectively. Notably, the dark zone in fig. 4(b) was anomalous eutectic structure. It could be seen that with the increase of initial undercooling, the volume fraction of anomalous eutectic increased gradually when the $Fe_{82}B_{17}Si_1$ eutectic alloy solidified in the undercooling range of 6—164 K. This also indicated that the undercooled anomalous eutectic was the product of the rapid solidification.

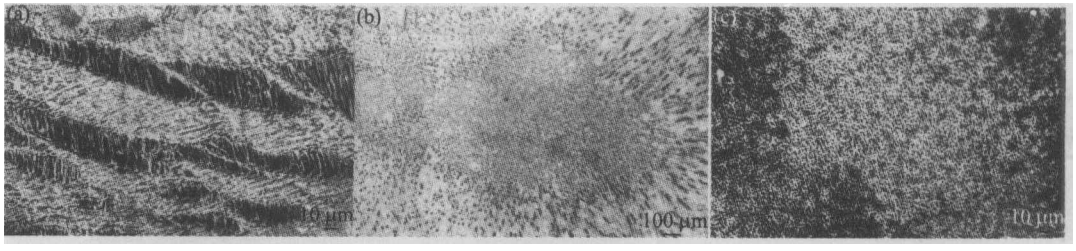

Fig. 4. Typical microstructures of $Fe_{82}B_{17}Si_1$ eutectic alloy with low magnification showing the dependence of volume fraction of anomalous eutectic on initial undercooling. (a) $\Delta T = 6$ K; (b) $\Delta T = 107$ K; (c) $\Delta T = 164$ K.

2.5 Coupled zone of α(Fe,Si)-Fe_2B eutectic system

Generally, the symmetric coupled zone is of eutectics involving two non-faceted phases, and the skewed-coupled zone is of eutectics formed by non-faceted phase and faceted phase under directional solidification condition[17]. Many experimental results have shown that there was not any primary α phase in the samples solidified below $\Delta T = 154$ K or above $\Delta T = 264$ K, whereas for the samples solidified in the initial undercooling range of 164—255 K there were always some volume fraction of primary α phase in their microstructures. These indicated that the boundary of the coupled zone of α(Fe,Si)-Fe_2B eutectic system shifted toward the Fe_2B side, and intersected the eutectic composition line at $\Delta T = 154$ K and $\Delta T = 264$ K, which was unlike the critical recalescence behavior with transforming points at $\Delta T = 164$ K and $\Delta T = 255$ K as shown in fig.1(b). This was because the character of the cooling curve could not be altered by the latent heat released during the rapid solidification of small volume fraction α phase at $\Delta T = 164$ K and $\Delta T = 255$ K. According to the results listed in table 1, it could also be inferred that the valley of the boundary line of the coupled zone was located at about $\Delta T = 207$K. According to the present experimental results, the schematic coupled zone of α

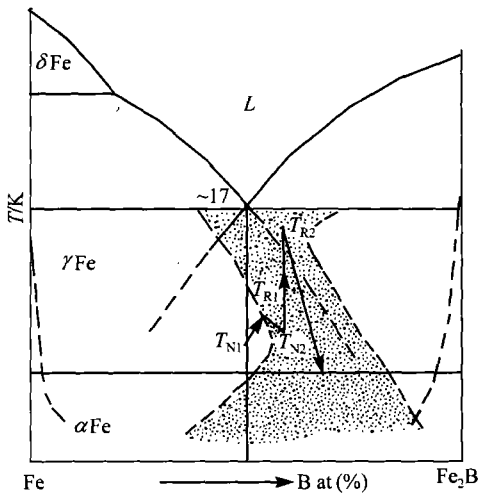

Fig. 5. The schematic coupled zone of α(Fe,Si)-Fe_2B eutectic system.

(Fe,Si)-Fe_2B eutectic system was shown as the shaded region in fig. 5, where ~ 17at% B was the equilibrium point of α(Fe,Si)-Fe_2B system and the dashed lines were the metastable liquidus and solidus ones below equilibrium temperature. Connecting the coupled zone of fig. 5 with the solidification microstructures and the cooling curves, the mechanism of microstructure formation in the undercooling range of 154—264 K could be considered as follows: when the melt was undercooled to T_{N1} accompanying the first recalescence, the α phase nucleated and grew rapidly in dendrite form. Meanwhile, B atoms accumulated in front of the α/L interface and impeded the growth of α phase. Samples entered the second cooling stage when the latent heat could no longer compensate the heat dissipated to the environment. The state (composition and temperature) of the melt around α phase varied from T_{N1} to the coupled zone as shown by the arrow in fig. 5. In addition, the accumulation of B atoms in front of the α/L interface also created the condition for Fe_2B to nucleate when the remaining melt cooled to T_{N2}. Since the nuclei of the two eutectic phases had formed, and Fe_2B phase could continuously catalyze α, the remaining melt grew in eutectic during the process of the second recalescence and thus formed the microstructure in figure. 3(c).

3 Conclusions

(i) By cyclic superheating incorporated with glass fluxing denucleation method the $Fe_{82}B_{17}Si_1$ eutectic alloy was undercooled up to $\Delta T = 342$ K ($0.238T_E$), which exceeded the formerly considered critical homogenous undercooling ($0.2T_E$).

(ii) For the samples solidified in the undercooling ranges of 6—164 K and 255—342 K, there was only one recalescence event on their cooling curves. Corresponding to the above two undercooling ranges the microstructures were mixed eutectic of quasi-regular and complex regular eutectic or mixed eutectic plus undercooled anomalous eutectic, and complete anomalous eutectic respectively, whereas for the samples solidified in the undercooling range of 174—247 K, two recalescence events occurred on the cooling curves, the microstructure corresponded to primary α(Fe, Si) plus interdendrite undercooled anomalous eutectic.

(iii) Two critical undercoolings were observed for undercooled $Fe_{82}B_{17}Si_1$ eutectic alloy: the mixed eutectic was the unique growth morphology when the undercooling was less than $\Delta T_1 = 63$ K; the microstructure transformed to complete undercooled anomalous eutectic when the undercooling was greater than $\Delta T_2 = 164$ K.

(iv) The two eutectic phases α(Fe,Si) and Fe_2B in the eutectic alloy conformed to the non-reciprocal nucleation effect, i.e. Fe_2B could catalyze the nucleation of α phase but α could not catalyze the Fe_2B to nucleate.

(v) The boundary of the coupled zone of α(Fe,Si)-Fe_2B eutectic system shifted toward the Fe_2B side, and intersected the eutectic composition line at ΔT = 154 K and ΔT = 264 K, whose valley was at about ΔT = 207 K.

References

1 Kattamis, T. Z., Flemings, M. C., Structure of undercooled Ni-Sn eutectic, *Metall Trans.*, 1970, 1(5): 1449.

2 Flemings, M. C., Shiohara, Y., Solidification of undercooled metals, *Mater. Sci. Eng.*, 1984, 65: 157.

3 Wu, Y., Piccone, T. J., Shiohara, Y. et al., Dendritic growth of undercooled nickel-tin: Part 1, *Metall. Trans.*, 1987, 18A(5): 915.

4 Piccone, T. J., Wu, Y., Shiohara, Y. et al., Dendritic growth of undercooled nickel-tin: Part 2, *Metall. Trans.*, 1987, 18A(5): 925.

5 Wu, Y., Piccone, T. J., Shiohara, Y. et al., Dendritic growth of undercooled nickel-tin: Part 3, *Metall. Trans.*, 1988, 19A(4): 1109.

6 Tewari, S. N., Effect of undercooling on the microstructure of Ni-35at pct Mo (eutectic) and Ni-38at pct Mo (hypereutectic) alloy, *Metall. Trans.*, 1987, 18A(3): 525.

7 Wei, B. B., Yang, G. C., Zhou, Y. H., High undercooling and rapid solidification of Ni-32.5 Sn eutectic alloy, *Acta. Metall. Mater.*, 1991, 39(6): 1249.

8 Wei, B., Herlach, D. M., Sommer, F. et al., Rapid dendritic and eutectic solidification of undercooled Co-Mo alloys, *Mater. Sci. Eng.*, 1994, A181/182: 1150.

9 Wei, B., Herlach, D. M., Sommer, F. et al., Rapid solidification of undercooled eutectic and monotectic alloys, *Mater. Sci. Eng.*, 1993, A173: 357.

10 Wei, B., Herlach, D. M., Sommer, F., Rapid eutectic growth of undercooled metallic alloys, *J. Mater. Sci. Lett.*, 1993, 12: 1774.

11 Ramanan, V. R. V., Fish, G. E., Cristallization kinetics in Fe-B-Si metallic glasses, *J. Appl. Phys.*, 1982, 53(3): 2273.

12 Raghavan, V., Phase Diagrams of Ternary Iron Alloys Part 6A, New Delhi: Electronic publishing center, 1991: 406—413.

13 Croker, M. N., Fidler, R. S., Smith, R. W., The characterization of eutectic structures, *Proc. R. Soc. London.*, 1973, 335A: 35.

14 Elliott, R., Eutectic solidification, *Mater Sci Eng*, 1984, 65: 85.

15 Kurz, W., Sahm, P. R., *Directional Solidified Eutectic Material* (transl. Li, X. L) Beijing: Publishing House of Metallurgical Industry, 1989: 70.

16 Sundquist, B. E., Mondolfo, L. F., Heterogeneous nucleation in the liquid-to-solid transformation in alloys, *Trans. Metall. of AIME.*, 1961, 221: 157—164

17 Bottinger, W. J., Growth kinetic limitations during rapid solidification, in *Rapidly Solidified Amorphous and Crystalline Alloys* (eds. Kear, B. H., Giessen, B. C., Cohen, M.), New York: Elsevier Science Publishing Co. Inc., 1982: 139.